

## Control and Exploitation of Thermal Distortions in Welded T-joints

Heikki Keinänen<sup>a</sup>, Jouni Alhainen<sup>a</sup>, Risto Karppi<sup>a</sup>, Martti Verho<sup>a</sup>

<sup>a</sup> Technical Research Centre of Finland (VTT), Finland, e-mail: *firstname.lastname@vtt.fi*

**Keywords:** Residual stresses, thermal distortions, welding deformations

### 1 ABSTRACT

The main objective of the DISCO (Control and Exploitation of Thermal Distortions) project performed in 2002-2004 was the creation of an overall concept for the control of thermal distortions. The domain of the project was limited to structural steels and to the processes most important to the participating industry.

The project explored the possibility to apply the inherent strain method for modelling thermal deformations by establishing an inherent strain database for major arc welding and thermal cutting situations. The project was executed in close co-operation with Osaka University, Japan, Lappeenranta University of Technology and four Finnish enterprises. The project included testing and modelling of welded T-joint and butt weld experiments with various plate thicknesses. The goal of the tests was to define an inherent strain database for the rather wide variety joint geometries.

The work focused on structural steels representing two strength levels, and several welding processes. The computational practices were revealed for treating thermal distortions. Further actions included testing and modelling of welded T-joint with various plate thicknesses.

The relationship between plastic strains and angular distortion of a fillet welded plate T-joints was studied using numerical analyses. A three dimensional thermo-elastic-plastic analysis incorporating the effects of a moving heat source and non-linear material properties was applied. Procedures to define inherent strain distribution and to compute deformations were presented.

The comparison of detailed thermo-elastic-plastic computation and measurements exhibited a good correlation. The simplified inherent strain type analysis underestimated somewhat the deformations.

### 2 INTRODUCTION

The thermo-elastic-plastic numerical analysis is gradually becoming a versatile tool for estimating and minimizing thermal distortions. The advances are not very rapid, however. Accordingly the great majority of these numerical solutions are still academic. Though several trials have been successfully made for industrial applications, they have been limited in scope to rather specific demonstrations only. The problems with this approach can be summarized as follows:

- Modelling and computation time is long for complicated structures;
- Data from performed simulations is insufficient for broader scope of applications;
- Good accuracy necessitates that material properties are known as a function of temperature;
- Many of the modern thermal processes and their process parameters have not been subjected to characterisation as heat sources for simulation purposes.

A summary of the computational welding simulation analyses can be found in Lindgren (2001a, b, c). The computational practices for treating thermal distortions have been revealed e.g. in reference Keinänen (2004). Application of inherent strain can be found e.g. in Gonghyun (2003), Hill (2001), Mochizuki (1999), and Wang (1998).

In this study the relationship between plastic strains and angular distortion (vertical deformation) of a fillet welded plate T-joints was studied using experiments and numerical analyses. A three dimensional thermo-elastic-plastic analysis incorporating the effects of a moving heat source and non-linear material properties was performed to obtain the plastic strain distributions and deformations. A further step was to apply a procedure that allows each plastic strain component enter the elastic model using equivalent thermal

strains. The deformation of the plate was estimated using linear elastic analysis. Finally, simplified plastic strain distributions (inherent strain) were derived and utilised in the same procedure.

The experimental results are reported by Alhainen (2006), and the computational analyses by Keinänen (2004a, 2004b).

### 3 COMPONENTS AND MATERIALS

The project comprised welding with MAG (Metal Active Gas Welding), FCAW (Flux Cored Arc Welding) and SAW (Submerged Arc Welding) methods. The plate thickness varied from 8 to 30 mm. In the case of T-joint the component web height was 150 mm, plate length was 600 mm and plate half-width was 300 mm.

Two constructional steels, S355J2G3 in conformity with standard EN 10025 and OPTIM RAEX 650 MC in conformity with standard EN 10113-3 were used. For the computation, the thermal and mechanical properties were estimated. The material properties were defined on the basis of literature as Metals Handbook (1990) and based on previous experience of similar computations, Heikinheimo (1999), and Keinänen (1998). Approximate values for the material properties were utilised, and phase transformations were not taken into account. The same material properties were used for the base and the weld material, as the filler metals substantially represented matching types.

The temperature dependent physical properties, conductivity and specific heat were utilised in the computation. The combined hardening material property parameters for Abaqus finite element computation were defined in such a way that the stress strain curves shown in Figure 1 were obtained.

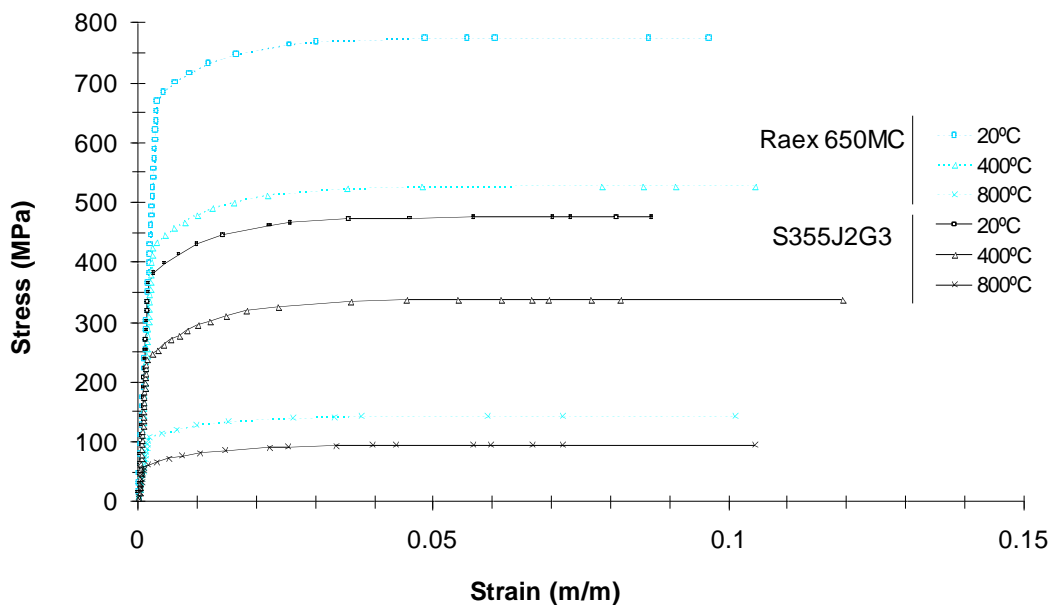


**Figure 1.** Engineering stress strain curves referred to at selected temperatures for the two materials studied

### 4 COMPONENT TESTS

The test results have been reported by Alhainen (2006). Laboratory scale experiments were carried out in order to define how the various welding processes (MAG, Tandem, FCAW and SAW) and welding parameters affect the distortions. Butt and T- welded joints and plate thicknesses of 8...30 mm were studied. Angular distortion was chosen as a target as the out-of-plane deformations are of major concern for rectification. The work included temperature measurements using thermocouples and dimensional measurements regarding to distortions.

The main deliverable of the tests was the data of dimensional measurements. The temperature measurements supported the model development together with the weld cross-section measurements. Thermal effect of welding was characterized for selected tests by monitoring the thermal cycles at several locations on the lower surface of the horizontal plate. The geometry of each component was assessed via accurate dimensional measurement before the welding test (tack welded specimen), after the first weld and

also after the second weld in a double fillet weld in T-joints. Figure 2 shows jugged welding test arrangement.



**Figure 2.** Jugged test arrangement

A few most interesting findings of the experiments were the following:

- Reduction of throat thickness is not always a panacea for reducing angular distortion. This type of deformation reaches its maximum when the plastic zone only just penetrates through the plate thickness. For instance with 8 mm thickness throat thickness of 5 mm causes larger deformations than 6 mm does;
- The last welded fillet in the double fillet weld in T-joint generally causes larger angular distortions than the first one. Submerged arc welding at smaller throat and plate thicknesses deviates from this behaviour;
- The increasing strength of the steel has a complex influence on the angular deformation: a decrease for fillet welds, ineffective for free butt joints, and an increase for butt joints that were released from heavy jugging after weld cooled down to room temperature.

## 5 NUMERICAL MODEL OF WELDED T-JOINT

Computation was performed for the majority of test cases. In the computation Abaqus code (version 6.4.3) was used, and thermal and mechanical analyses were performed separately. The first, baseline computation was performed for the test A2 (plate thickness 8 mm). Combined hardening material model and small strains and displacements were utilised.

Before the final model, several pre-runs with different mesh divisions were performed. Figure 3 shows the finite element model, referred to as the large model.

In the case of the T-joint a gap between the web and flange was modelled without contact conditions. In the computation the weld material was incorporated into the model using the Abaqus “model change” option. In the mechanical analysis double weld elements were used. The first set was modelled with soft material properties, and the goal was to track the accumulated deformation of the nodes. Just before weld element activation, these elements were removed from the model. The actual weld elements were added to the model in a strain free state.

In the model the nodes corresponding to two lines in the welding direction and at a distance of 50 mm from the outer edges of the plate were fixed in the vertical direction to model the support condition of the test specimen. Additional displacements of selected nodes in the direction of the remaining coordinate axes were fixed to prevent rigid body movement.

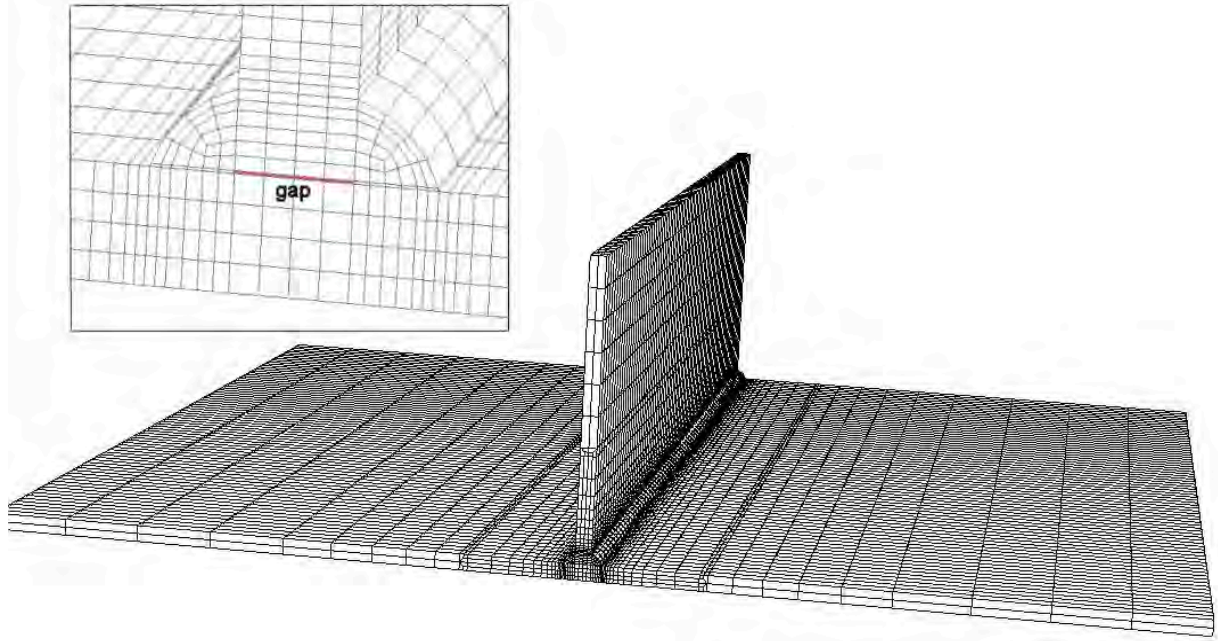


**Figure 3.** Large finite element model

In the thermal analysis heat input was modelled using uniform internal heat generation (heat generation was uniform in an area selected based on previous experience) and a sinusoidal time function. The amount of heat input ( $Q$ , (J/s)) was obtained using the welding parameters and thermal efficiency ( ) of 80 % as

$$Q = \eta \times U \times I \quad (1)$$

where  $U$  is voltage (V) and  $I$  is current (A).

To limit computation time, a model with reduced length was constructed. A length of 150 mm (instead of 600 mm) was modelled. The planes transverse to the welding direction were forced to remain planar. Otherwise the boundary conditions were similar to those of the large model. In the reduced model the weld and base material had coincident but separate nodes. In the analysis the displacements of these coincident nodes were forced to be equal. This procedure was performed to separate the strains in the base and in the weld material. More elements were generated near the weld area to get more accurate prediction of the plastic strains. Tack welds were not modelled. A specific code was made to vary the plate and weld dimensions in order to realise the computation of the experiments. Cooling was accelerated in the reduced (short) model using convection boundary conditions to prevent for over heating.

## 6 SIMPLIFIED DISTORTION ANALYSIS

The goal was to obtain simplified inherent strain distribution so that the deformation can be still predicted with a reasonable accuracy.

The basic idea related to the inherent strains is, that the welding-induced distortions can be predicted by utilising the computed plastic strains. Each plastic strain component is used to predict distortion using an elastic model. Here temperature and the corresponding thermal expansion coefficient were used to model initial strain field in a linear elastic model. To separate the effects of each strain component, orthotropic material model was utilised. The plastic strain was converted to thermal expansion coefficient as

$$\epsilon_i = \alpha_i / (T - T_{ref}) \quad (2)$$

where  $\epsilon_{pi}$  is the  $i$ :th component of plastic strain,  $\alpha_i$  is thermal expansion coefficient,  $T$  is temperature (value of 1.0 °C was selected for  $T$ ) and  $T_{ref}$  is reference temperature (= 0 °C).

## 7 RESULTS

The results for two T-joint experiments, A2 and I1, are presented here.

### 7.1 Thermal results

Table 1 summarizes the welding parameters and Table 2 the thermal results for the considered T-joint experiments. In both case the material was S355J2G3.

**Table 1.** Welding parameters for experiments A2 and I1

Experiment	Plate thickness (mm)	Current (A)	U (V)	V (mm/s)	Heat Input (kJ/mm)
A2	8	253	29.2	5.8	1.3
I1 (tandem)	12	608 (1)	28.1 (1)	9.2	1.9
		634 (2)	27.1 (2)		

**Table 2.** Thermal results (temperature (°)) for experiments A2 and I1. The distance of the location of interest is either 0 mm or 20 mm (see Figure 4).  $t_{8/5}$  is time which is needed to cool down from 800 to 500 °C.

Experiment	$T_{max}/0mm$		$T_{max}/20mm$		$t_{8/5}$ (s)	
	Measured	Computed	Measured	Computed	Measured	Computed
A2	554	662	315	295	10	10.4
I2-tandem	-	535	-	351	-	16.1

Figures 4 and 5 show comparison of computed and measured temperatures at three locations at the lower surface of the plate for the experiments A2 and I1.

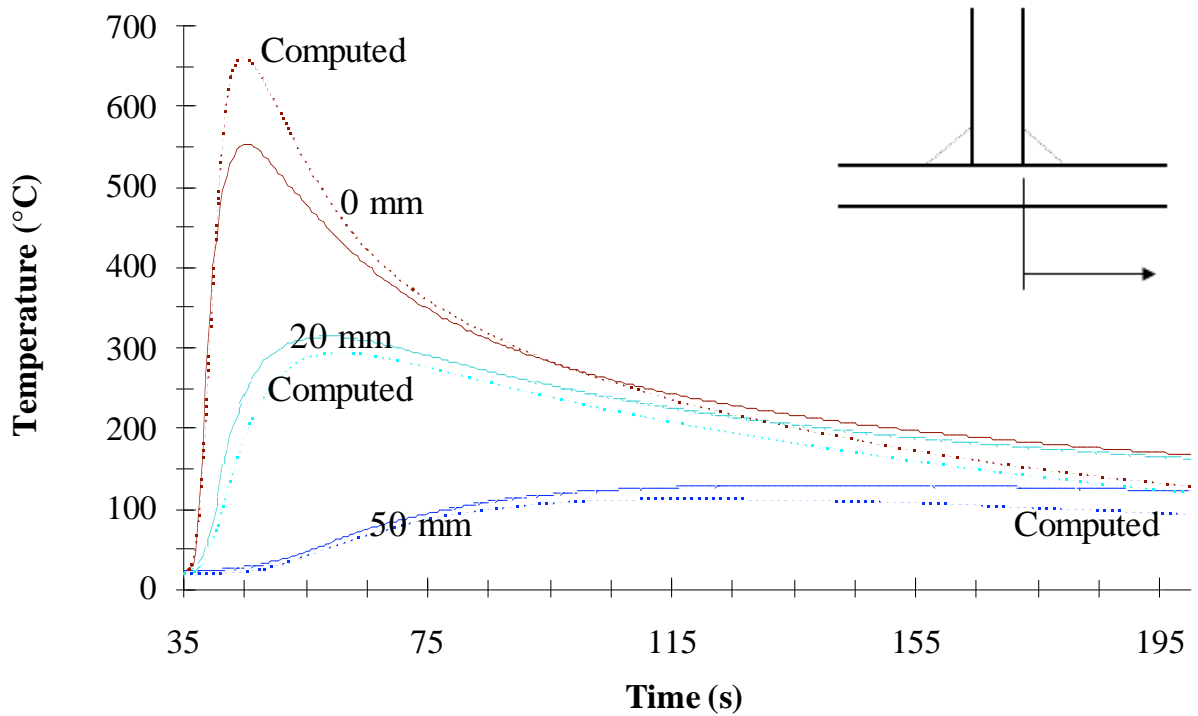


**Figure 4.** Comparison of computed and measured temperatures, experiment A2

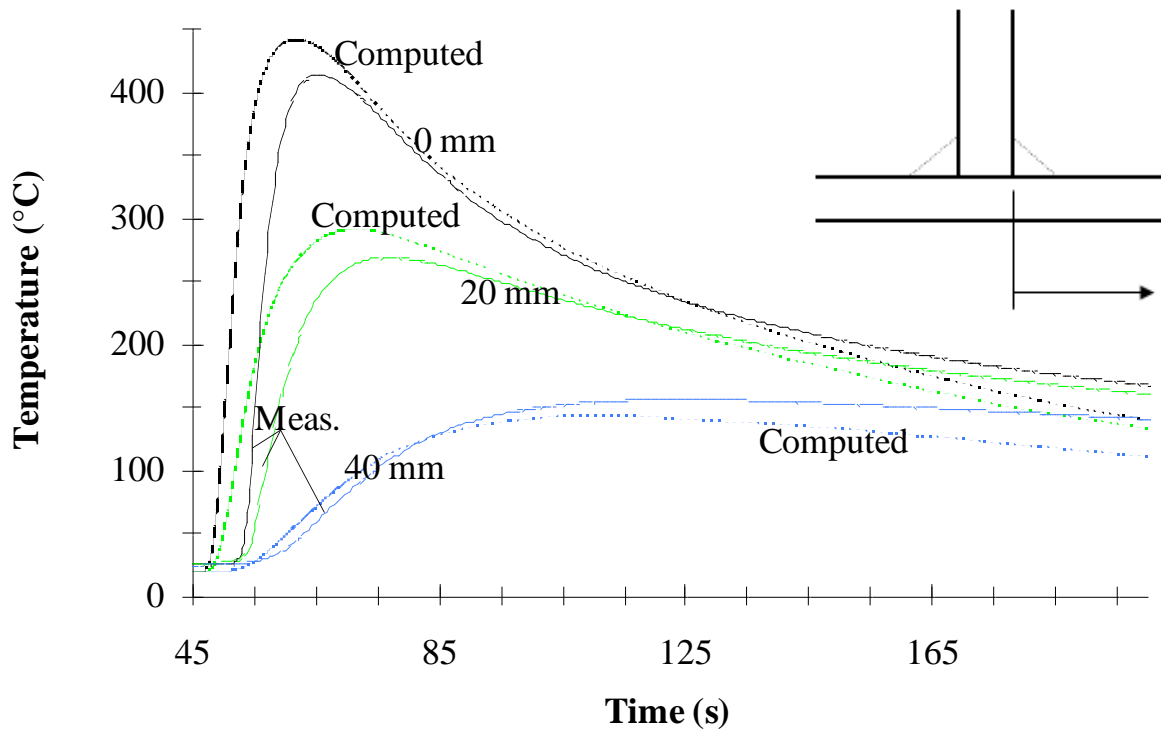


**Figure 5.** Comparison of computed and measured temperatures, experiment I1

The computation predicts rather well the measured temperatures. Some differences can be found especially in terms of maximum values of temperature. In addition temperatures at larger time values are not so well predicted due to the short model and its boundary conditions.

From the polished cross sections the fusion line and the heat affected zone was estimated. This allowed the corresponding isotherms to be identified and compared to computed ones. Although the overall correspondence was reasonably good, some differences existed in the penetration depth and in the shape of the zones.

## 7.2 Mechanical results

In the studied T-joints the angular deformation prevails among the six different kinds of weld distortion. The flange is slightly rotated, but the overall longitudinal bending deformation remains small. In the case of the short model, the longitudinal effects, even they are small, could not be predicted.

Figure 6 shows computed von Mises stress distribution after welding and cooling down for the experiment A2. Table 3 compares measured and computed deformations in the middle of the plate for the both cases. The correspondence between computed and measured deformations is good. The angular deformation results of the reduced model coincide nicely with those of the large model, Keinänen (2004b).

**Table 3.** The measured and computed (reduced model) deformations (mm) for the experiments A2 and I1.

Experiment	measured	computed
A2	8.1	9.2
I1	7.3	5.8

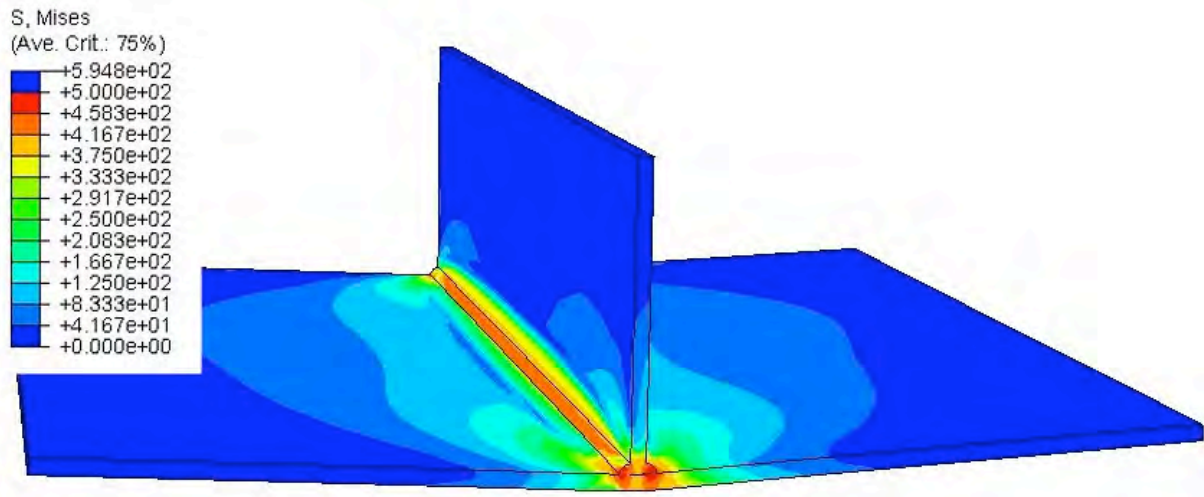


**Figure 6.** Computed residual von Mises stress (MPa) distribution, large model, experiment A2

### 7.3 Evaluation of inherent strain

The transverse tensile and shear strain components were shown to have the greatest influence on the angular deformation (Keinänen (2004a, 2004b)). The goal was to obtain simplified inherent strain distribution from the computed plastic strains. Transverse tensile and shear plastic strain components were integrated over the transverse coordinate (-15...+15 mm). Using these integrated values, an intermediate strain value was produced corresponding to depths  $0 \dots \frac{1}{4} \cdot t$  mm,  $\frac{1}{4} \cdot t \dots \frac{t}{2}$  mm,  $\frac{t}{2} \dots \frac{3}{4} \cdot t$  mm and  $\frac{3}{4} \cdot t \dots t$  mm ( $t$  is plate thickness). Figure 7 shows the computed transverse plastic strain different depths in the plate (transverse coordinate at the weld centreline = 0 mm) in the case of the experiment A2. The integrated transverse tensile and shear strain components are shown in Table 4 for the experiments A2 and I1.

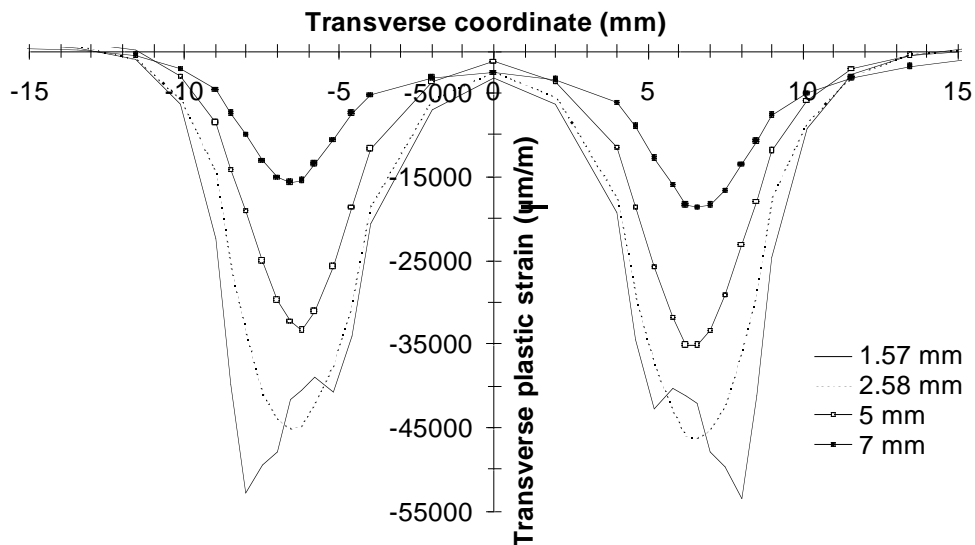


**Figure 7.** The computed transverse plastic strain at different depths in the plate (value of the transverse coordinate at the weld centreline = 0 mm), experiment A2

The strains presented in Table 4 were utilised to computed deformations with the model shown in Figure 8. A simplified distortion analysis (Chapter 6) was performed, and the computed deformations for the experiments were: 7.5 mm/A2, 5.4 /I1. These values are slightly lower than the computed values presented in Table 3. Finally, an illustrative trial was made to apply this kind of computation to an industrial case (Verho 2006).

**Table 4.** The integrated strain values corresponding to depths  $0 \dots \frac{1}{4}t$  mm,  $\frac{1}{4}t \dots \frac{t}{2}$  mm,  $\frac{t}{2} \dots \frac{3}{4}t$  mm and  $\frac{3}{4}t \dots t$  mm ( $t$  is plate thickness). The results were integrated over a width of  $\pm 15$ mm.

Test name	Width (mm)	Depth (mm)	Transverse strain ( m/m)		Shear strain ( m/m)		
			weld bead nr 1	2	weld bead nr 1	2	
<b>A2</b>	1	0...15	0...2	-18154	-18028	-39949	-39443
	2	0...15	2...4	-14278	-13805	-2347	-1910
	3	0...15	4...6	-10450	-9704	-1366	-1220
	4	0...15	6...8	-6691	-5702	-687	-766
<b>I1</b>	1	0...15	0...3	-6637	-6849	-40144	-40050
	2	0...15	4...6	-3772	-3921	-446	-460
	3	0...15	6...9	-1137	-1279	-248	-284
	4	0...15	9...12	966	907	-130	-150

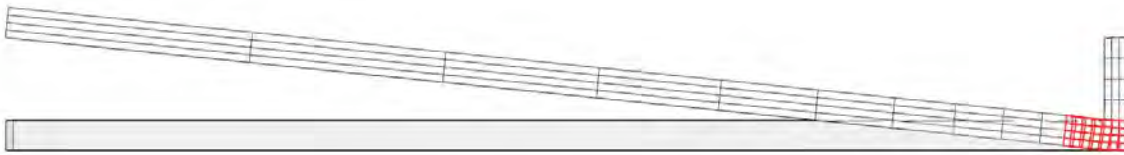


**Figure 8.** The simple model to compute deformations using strains presented in Table 4. Model width is 300 mm

## 8 CONCLUSION

The relationship between plastic strains and angular distortion (vertical deformation) of a fillet welded plate T-joints was revealed using numerical analyses. A three dimensional thermo-elastic-plastic analysis incorporating the effects of a moving heat source and non-linear material properties was performed to obtain the plastic strain distributions and deformations. Moreover, a procedure in which each plastic strain component was entered into elastic model as an initial strain was introduced and utilised.

The procedure to define the simplified strain distribution (inherent strain) was presented. The deformation of the plate was also estimated using this strain distribution.

The comparison of detailed thermo-elastic-plastic computation and measurements exhibited a good correlation. The temperatures were rather well predicted. Due to the reduced model ( $\frac{1}{4}$  length was modelled) and related boundary conditions cooling at larger time values could not be accurately modelled. The thermal zones could be reasonable well modelled, although the depth and the form of penetration in the computation deviated in some cases from the real one. A more detailed heat input model, e.g. double ellipsoidal, would probably improve the computational results. However, the computational work would increase.

The angular deformation could be rather well modelled, although the reduced length model and the simplified heat input model caused some differences between computed and measured deformations. The tandem weld case could be rather well modelled in terms of compatibility with thermal and mechanical test results. The simplified inherent strain type analysis underestimated somewhat the deformations. The following details should be further considered in the future:

- More advanced modelling of the heat input in the detailed finite element computation
- Effect of the boundary conditions on the results. So far only free conditions, i.e. without any external constraints (except the plate stiffness) have been studied.
- More specific determination of material properties, consideration of weld properties.
- In the simplified analysis the plastic strains in the weld and in the vertical plate were not taken into account. The integration of the plastic strains and the simplified modelling should be also further developed.

- Construction of an inherent strain database corresponding to different welding methods, boundary conditions and geometries should be possible on the basis of the presented results.

**Acknowledgements.** *This work belongs to the DISCO (Control and Exploitation of Thermal Distortions) project led by VTT Industrial Systems and funded by National Technology Agency of Finland (TEKES) with following participating and funding industrial and other organisations: John Deere Forestry Oy (former Timberjack Oy), Steelpolis, Rautaruukki Oyj, Lappeenranta University of Technology and VTT. This presentation has been prepared under the SAFIR/FRAS research project, which concern integrity of the reactor circuit and its component. The project is a part of SAFIR2010, which is a national nuclear energy research program funded by the Teollisuuden Voima Oy (TVO), the State Nuclear Waste Management Fund (VYR) and the Technical Research Centre of Finland (VTT).*

## REFERENCES

Abaqus 6.4.3. Abaqus Inc. 2003.

Alhainen, J., Karppi, R. & Keinänen, H: 2006. Experimental study on thermal deformations caused by welding and cutting. Research Report no. VTT-R-04569-06, Espoo, Finland.

Gonghyun Jung, B.S. 2003. Plasticity-based distortion analysis for fillet welded thin plate t-joints. Dissertation, School of The Ohio State University, 2003.

Heikinheimo, L. 1999. Material properties for assessment of thermal residual stresses. Report VALB360. VTT Manufacturing Technology, Espoo, Finland, 1999. 20 p.

Hill, M. R. 2001. Modelling of residual stress effects using eigenstrain. ICF10979OR, 10th Inter. Conference on Fracture, Oahu, Hawaii, 12/2001.

Keinänen, H. 1998. Welding residual stresses in a thick nozzle joint. Baseline analysis of the Work Package 3 of the "Variation of Residual Stresses in Aged Components (VORSAC)" - project. VTT Manufacturing Technology, Espoo 1998. VTT-VALC535. 33 + 8 p. VORSAC(99)W037 (confidential).

Keinänen, H. Karppi, R. 2004. Computational practices for prediction of thermal distortions. Research report no. TUO72-044621, VTT Industrial Systems, Espoo, Finland. 21 p.

Keinänen, H. Karppi, R. 2005a. Computation of welding deformations of a T-joint. Baseline computation of the DISCO experiments. Research report no. TUO72-055743. VTT, Espoo, Finland. 26 p.

Keinänen, H. Karppi, R. 2005b. Computation of welding deformations of "DISCO" T-joint and butt welding experiments. Research report no. TUO72-056607. VTT, Espoo, Finland. 26 p.

Lindgren, L.E. 2001a. Finite element modelling and simulation of welding part 1: Increased complexity. Journal of Thermal Stresses, 24:141-192, 2001. 0149-5739/01.

Lindgren, L.E. 2001b. Finite element modelling and simulation of welding part 2: Improved material modelling. Journal of Thermal Stresses, 24:195-231, 2001. 0149-5739/01.

Lindgren, L.E. 2001c. Finite element modelling and simulation of welding part 3: Efficiency and integration. Journal of Thermal Stresses, 24:305-334, 2001. 0149-5739/01

Mochizuki, M. & Toyoda M. 1999. Numerical analysis of residual stress in welded structures using inherent strain. Pp. 549-580. Mathematical Modelling of Weld Phenomena 5. Proceedings of the 5th International Seminar on the Numerical Analysis of Weldability. Graz-Seggau, 4 - 6 October 1999.

Metals Handbook, Volume 1. Properties and Selection: Irons, Steels, and High performance Alloys, 10th ed. Eds. Davis, J. R. et al. ASM International USA, 1990. 1063 p.

Verho, M. & Karppi, R. 2006. Demonstration of the application of a simplified method to define welding deformations in an industrial case. VTT Research Report TUO72-056608. VTT, Espoo, Finland.

Wang J., Lu H., Murakawa, H. & Luo, Y. 1998. Prediction of welding deformations by FEM based on inherent strains. Modelling of casting, welding and advanced solidification processes VIII. Edited by B.G. Thomas and C. Beckermann. The Minerals, Metals and Materials Society. p. 803-810.